Institut für Computergraphik und Algorithmen
Technische Universität Wien

Karlsplatz 13/186/2
A-1040 Wien
AUSTRIA

Tel: +43 (1) 58801-18601
Fax: +43 (1) 58801-18698

Institute of Computer Graphics and Algorithms
Vienna University of Technology

email:
technical-report@cg.tuwien.ac.at

other services:
http://www.cg.tuwien.ac.at/
ftp://ftp.cg.tuwien.ac.at/

Combined Rendering of Polarization and Fluorescence Effects

Alexander Wilkie, Robert F. Tobler, Werner Purgathofer

TR-186-2-01-11
April 2001

Abstract

We propose a practicable way to include both polarization and fluorescence effects in a rendering system at the same time. Previous research in this direction only demonstrated support for either one of these phenomena; using both effects simultaneously was so far not possible, mainly because the techniques for the treatment of polarized light were complicated and required rendering systems written specifically for this task.
The key improvement over previous work is that we use a different, more easily handled formalism for the description of polarization state, which also enables us to include fluorescence effects in a natural fashion. Moreover, all of our proposals are straightforward extensions to a conventional spectral rendering system.

Keywords: polarization, fluorescence, predictive rendering

1 Introduction

For the purposes of truly predictive photorealistic rendering it is essential that no effect which contributes to the interaction of light with a scene is neglected. Most aspects of object appearance can be accounted for by using just the laws of geometric optics, comparatively simple descriptions of surface reflectivity, tristimulus representations of colour and light, and can nowadays be computed very efficiently through a variety of common rendering algorithms. However, several physical effects, namely fluorescence, diffraction, dispersion and polarization, are still rarely – if at all – supported by contemporary rendering software.

1.1 Polarization

Polarization has received particularly little attention because – while of course being essential for specially contrived setups that e.g. contain polarizing filters – it seemingly does not contribute very prominent effects to the appearance of an average scene. This misconception is in part fostered by the fact that the human eye is normally not capable of distinguishing polarized from unpolarized light[1].
One of the main areas where it in fact does make a substantial difference are outdoor scenes; this is due to the usually quite strong polarization of skylight, as one can find documented in G. P. Können's book [6] about polarized light in nature. But since such scenes are currently still problematical for photorealistic renderers for a number of other, more obvious reasons (e.g. scene complexity and related global illumination issues), this has not been given a lot of attention yet. Other known effects which depend on polarization support are certain darkening or discolourization patterns in metal objects and their reflections, and the darkening of certain facets in transparent objects such as crystals.

1.2 Fluorescence

Some of the reasons for the small amount of work fluorescence has received are different from those which have made polarization a fringe topic. Firstly, although it causes very prominent effects, these can also be faked comparatively easily through custom shaders at a fraction of the effort involved in actually simulating the real process. Secondly, measurements of fluorescent pigments are very hard to obtain, virtually no publicly accessible data of this kind exists, and designing such spectra by hand is tedious. The third main reason is shared between fluorescence and polarization: they ought to be done using a spectral rendering system, which still rank as comparatively exotic and expensive to use.

2 Background

In this section we discuss three topics: we give a brief overview of the physics behind the phenomena of polarized light and of fluorescence, and we recapitulate the workings of a particular ubiquitous raytracing acceleration technique, since this has implications on how polarization support ought to be implemented in a rendering system.

[1] Contrary to common belief trained observers *can* distinguish polarized from unpolarized light with the naked eye. Named after its discoverer, the effect is known as *Haidinger's brush* and is described by Minnaert in his book about light in outdoor surroundings [7].

2.1 Polarized Light

While for a large number of purposes it is sufficient to describe light as an electromagnetic wave of a certain frequency that travels linearly through space as a discrete ray (or a set of such rays), closer experimental examination reveals that such a wavetrain also oscillates in a plane perpendicular to its propagation. The exact description of this phenomenon requires more than just the notion of radiant intensity, which the conventional representation of light provides.

The nature of this oscillation can be seen from the microscopic description of polarization, which closely follows that given by Shumaker [11]. We consider a single steadily radiating oscillator (the light source) at a distant point of the negative Z–axis, and imagine that we can record the electric field[2] present at the origin due to this oscillator. Except at distances from the light source of a few wavelengths or less, the Z component of the electric field will be negligible and the field will lie in the X–Y plane. The X and Y field components will be of the form

$$\begin{aligned} E_x &= V_x \cdot (2\pi \cdot \nu \cdot t + \delta_x) \quad [\mathrm{V} \cdot \mathrm{m}^{-1}] \\ E_y &= V_y \cdot (2\pi \cdot \nu \cdot t + \delta_y) \end{aligned} \tag{1}$$

where V_x and V_y are the amplitudes $[\mathrm{V} \cdot \mathrm{m}^{-1}]$, ν is the frequency [Hz], δ_x and δ_y are the phases [rad] of the electromagnetic wavetrain, and t is the time [s]. Figure 1 illustrates how this electric field vector E changes over time for four typical configurations.

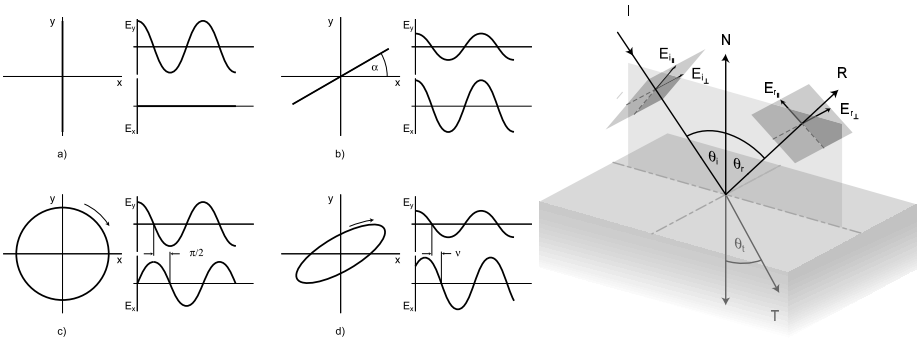

Fig. 1. Left: Four examples of the patterns traced out by the tip of the electric field vector in the X–Y plane: a) shows light which is linearly polarized in the vertical direction; the horizontal component E_x is always zero. b) is a more general version of linear polarization where the axis of polarization is tilted by an angle of α from horizontal, and c) shows right circular polarized light. The fourth example d) shows elliptically polarized light, which is the general case of equation (1). (Image redrawn from Shumaker [11]) **Right:** Geometry of a ray–surface intersection with an optically smooth phase boundary between two substances, as described by the equation set (2). A transmitted ray T only occurs in when two dieelectric media interface; in this case, all energy that is not reflected is refracted, i.e. $T = I - R$. The E–vectors for the transmitted ray $\mathrm{E}_{t_{\|}}$ and $\mathrm{E}_{t_{\perp}}$ have been omitted for better picture clarity. The $(\mathrm{E}_{\|}, \mathrm{E}_{\perp})$ components here correspond to the (x, y) components in the drawing on the left.

Causes of Light Polarization. Apart from skylight, it is comparatively rare for light to be emitted in polarized form. In most cases, polarized light is the result of interaction with

[2] The electric and magnetic field vectors are perpendicular to each other and to the propagation of the radiation. The discussion could equally well be based on the magnetic field; which of the two is used is not important.

transmitting media or surfaces. The correct simulation of such processes is at the core of predictive rendering, so a short overview of this topic recommends itself.
The simplest case is that of light interacting with an optically smooth surface. This scenario can be adequately described by the *Fresnel equations*, which are solutions to Maxwell's wave equations for light wavefronts. They have been used in computer graphics at least since Cook and Torrance proposed their famous reflectance model [2], and most applications use them in a form which is simplified in one way or another.

Fresnel Terms. In their full form (the derivation of which can e.g. be found in [12]), they consist of *two* pairs of equations. According to the reflection geometry in figure 1, the first pair determines the proportion of incident light which is reflected separately for the *x* and *y* components of the incident wavetrain. This relationship is commonly known, and can be found in numerous computer graphics textbooks.
The second pair, which is much harder to find in computer graphics literature, descibes the *retardance* that the incident light is subjected to, which is the relative phase shift that the vertical and horizontal components of the wavetrain undergo during reflection. In figure 2 we show the results for two typical materials: one conductor, a class of materials which has a complex index of refraction and is always opaque, and one dieelectric, which in pure form is usually transparent, and has a real–valued index of refraction.
We quote the Fresnel equations for a dieelectric–complex interface. This is the general case, since only one of two media at an interface can be conductive (and hence opaque), and a dieelectric–dieelectric interface with two real–valued indices of refraction can also be described by this formalism.

$$
\begin{aligned}
F_\perp(\theta,\eta) &= \frac{a^2+b^2-2a\cos\theta+\cos^2\theta}{a^2+b^2+2a\cos\theta+\cos^2\theta} \\
F_\parallel(\theta,\eta) &= \frac{a^2+b^2-2a\sin\theta\tan\theta+\sin^2\theta\tan^2\theta}{a^2+b^2+2a\sin\theta\tan\theta+\sin^2\theta\tan^2\theta}F_\perp(\theta,\eta) \\
\tan\delta_\perp &= \frac{2\cos\theta}{\cos^2\theta-a^2-b^2} \\
\tan\delta_\parallel &= \frac{2b\cos\theta[(n^2-k^2)b-2nka]}{(n^2+k^2)^2\cos^2\theta-a^2-b^2} \\
&with \\
2a^2 &= \sqrt{(n^2-k^2-\sin^2\theta)^2+4n^2k^2}+n^2-k^2-\sin^2\theta \\
2b^2 &= \sqrt{(n^2-k^2-\sin^2\theta)^2+4n^2k^2}-n^2+k^2+\sin^2\theta
\end{aligned}
\tag{2}
$$

$F_\parallel$ is the reflectance component parallel to the plane of incidence, and $F_\perp$ that normal to it. Under the assumption that one is only interested in the radiant intensity of the reflected light, this can be simplified to the commonly used average reflectance $F_{average} = (F_\perp + F_\parallel)/2$. $\delta_\perp$ and $\delta_\parallel$ are the retardance factors of the two wavetrain components.

2.2 Fluorescence

While the polarization of light at a phase boundary is a comparatively macroscopic phenomenon, fluorescence is caused by processes within the pigment molecules that are responsible for the colour of an object. Due to both lack of space, and the fact that an actual

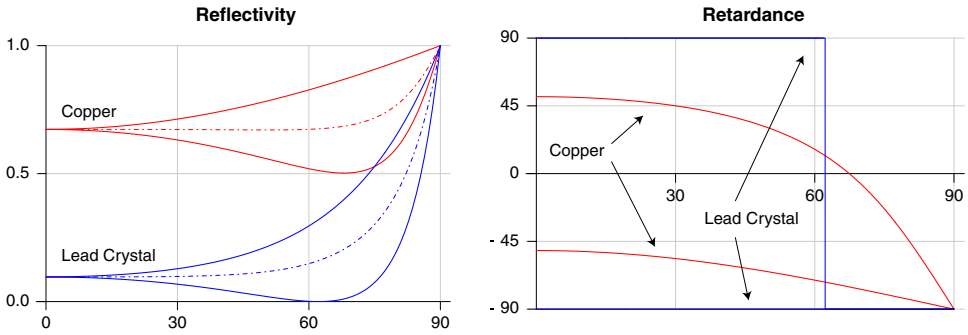

Fig. 2. Fresnel reflectivities $F_{\parallel}$, $F_{\perp}$ and $F_{average}$ (dashed lines), as well as parallel and perpendicular retardance values for copper (red) and lead crystal (blue) at 560nm. As a conductor, copper has a complex index of refraction, does not polarize incident light very strongly at Brewster's angle and exhibits a gradual shift of retardance over the enitre range of incident angles. For lead crystal, with its real–valued index of refraction of about 1.9, total polarization of incident light occurs at about 62°. Above this angle, no change in the phase relation of incident light occurs (both retardance components are at $-90°$), while below Brewster's angle a phase difference of 180° is introduced.

explanation of these processes is not necessary to properly implement support for it in a rendering system, we will not go into details about its causes.
The results of the phenomenon – which are what we try to simulate – are quite straightforward to describe: the characteristic property of fluorescent materials is that they re–emit portions of the incident light at different, lower wavelengths within an extremely short time (typically 10^{-8} seconds).
Instead of the reflectance spectra used for normal pigments, describing such a material requires knowledge of its *re–radiation matrix*, which encodes the energy transfer between different wavelengths. Such *bispectral* reflectance measurements are rather hard to come by; while "normal" spectrophotometers are becoming more and more common, the bispectral versions of such devices are by comparison very rare and in an experimental stage. Figure 3 shows three visualizations of a sample bispectral reflectance dataset.
Manual design of such re–readiation matrices is much harder than explicit derivation of reflection spectra; while the latter is already not particularly easy, their effect is by comparison still quite predictable. Also, it is easy to maintain the energy balance of normal reflection spectra by ensuring that no component is greater than one; for a re–readiation matrix this translates to the more difficult condition that the integral over the area must not exceed one.

2.3 Raytracing with Adaptive Tree–Depth Control

Historically, the introduction of recursive raytracing by Whitted [15] can be considered one of the major breakthroughs in the use of ray–based image synthesis methods. Subsequent work addressed performance optimization of such renderers; one key contribution in this area was the proposal of Hall and Greenberg [4] to adaptively prune the tree of recursive intersections for a given sample point, a technique which is in such widespread use nowadays that it is usually taken for granted.
Instead of recursively tracing reflections to a given recursion depth and simply adding the contributions of all successive ray intersections, they suggested to consider the possible maximum contribution of child rays (the so–called *ray weight*) to a sample point, and to

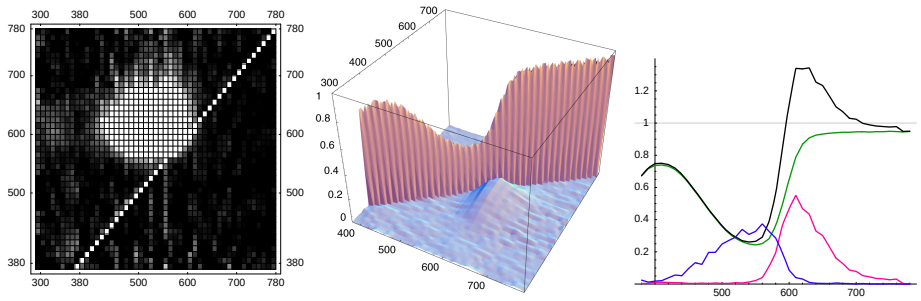

Fig. 3. Bispectral reflectivity measurements of pink fluorescent 3M Post-It®notes. The re–radiation matrix is shown for excitation wavelengths between 300nm and 780nm, and emission wavelengths from 380nm to 780nm, as 2D density plot and 3D graph. In the 3D view the off–axis contribution had to be exaggerated in order to be properly visible, and in both plots measurement noise is evident. The rightmost graph shows the nonfluorescent reflection spectrum (the main diagonal of the re–radiation matrix, shown in green), the energy absorbed at higher wavelegths (blue), the energy re–radiated at lower wavelengths (red) and the resulting "reflection" spectrum (black). Note that the resulting spectrum is well over 1.0 in some areas. Data courtesy of Labsphere Inc.

stop the recursion if it is below a certain threshold. This enables the early elimination of recursive rays that cannot contribute significantly enough to the final image, and leads to substantial performance gains.

Light and Filters. The key implication of this technique is that the contribution of a surface intersection (stored in the ray weights) has to be considered separately from the light ray which is modified by it. A different, and in our context more intuitive, term for a ray weight is *filter*; this is suggestive of the fact that for a particular intersection geometry the weight actually encodes the filtering attenuation of a light ray that comes in contact with the surface in question.
Using this approach has been a standard implementation technique for almost as long as raytracing has been in widespread use. However, the fact that almost all rendering systems use tristimulus colour values to describe both surfaces and light (and of course ignore more sophisticated physical effects) has obscured the fact that ray weights – or filters – and light are actually *separate entities*.
We mention this here because the – usually tacitly assumed – symmetry between light and filters is broken if either polarization or fluorescence are to be considered in a rendering system; as we will see, one can no longer use the same data structures to encode the two.

3 Previous Work

3.1 Raytracing with Polarization Parameters

There are two publications in computer graphics literature about this topic; one by Wolff and Kurlander [16], who demonstrated the concept for the first time, and one by Tannenbaum et al. [14], who concentrated on the rendering of anisotropic crystals and extended the techniques used by Wolff et al.
The main goal of these efforts was that of finding an appropriate way to describe, and perform calculations with, polarized light; both groups of authors settled for a notation

suggested by standard reference texts from physics literature.

Coherency Matrices. The formalism to describe polarized light used by both Wolff and Tannenbaum is that of *coherency matrices* (CM for short); this technique was introduced by Born and Wolf [1]. Similar to the discussion in section 2.1, one considers a monochromatic wave propagating along the positive Z–axis, and treats the E–field vector as consisting of two orthogonal components in X and Y directions. The phase relationships between the two can exhibit anything between full correlation (fully coherent or polarized light) to totally uncorrelated behaviour (incoherent or unpolarized light). As derived in detail by Tannenbaum et al. [14], the coherency state of such a monochromatic wave can be expressed in a matrix J of the form

$$J = \begin{pmatrix} J_{xx} & J_{xy} \\ J_{yx} & J_{yy} \end{pmatrix} = \begin{pmatrix} \langle E_x E_x^\star \rangle & \langle E_x E_y^\star \rangle \\ \langle E_y E_x^\star \rangle & \langle E_y E_y^\star \rangle \end{pmatrix}$$

where E_x and E_y are the time average of the E–field vectors for the X and Y directions, respectively, and $E_x^\star$ denotes the complex conjugate of E_x. The main diagonal elements – J_{xx} and J_{yy} – are real valued, and the trace $T(J)$ of the matrix represents the total light radiation of the wave, while the complex conjugates J_{xy} and J_{yx} represent the correlation of the X and Y components of E. For fully polarized light, these components are fully correlated and $|J|$ vanishes.
It is worth noting that coherency matrices – while they might seem rather different at first glance – encode the same information as equation (1). Born and Wolf [1] also discuss how one can compute the elements of a coherency matrix from actual irradiance measurements, which is an important point if one wants to eventually validate computer graphics models that use polarization in their calculations.

Coherency Matrix Modifiers. Besides being able to describe a ray of light, it is also necessary to process the interaction of light with a medium, as outlined in section 2.3. Such filtering operations on polarized light described by a coherency matrix can be performed by using *coherency matrix modifiers*, or CMM. Tannenbaum et al. brought this approach, which was originally introduced by Parrent et al. [8], to the computer graphics world for use in their rendering system.
CMMs have the form of a real–valued 4×4 matrix. If all participating elements have the same reference coordinate system, such matrices can be applied to a given coherence matrix J in the sequence of $J_p = \mathcal{M}_p J \mathcal{M}_p^\dagger$, where $\mathcal{M}_p^\dagger$ signifies the conjugate transpose of $\mathcal{M}_p$. If the modifier and the coherency matrix are not in the same coordinate system, an appropriate transformation – as discussed in section 2.3 of Tannenbaum et al. [14] – has to be applied first.

3.2 Reflection Models which take Polarization into Account

Apart from the case of perfect specular reflection and refraction, which is already adequately covered by the Fresnel terms discussed in section 2.1 and the modified Cook–Torrance model used by Wolff et al., only one other surface model proposed so far, namely that of He et al. [5], attempts to consider polarization effects. As could be inferred from the results section of this paper, the high complexity of their surface model apparently led the authors to only implement a simpler, non–polarizing version in practice, and to contain themselves with just providing the theoretical derivation of the polarization–aware model in the text.

3.3 Rendering of Fluorescence Effects

So far Glassner has apparently been the only graphics researcher who investigated the rendering of fluorescence phenomena [3]. The main focus of his work was centered around the proper formulation of the rendering equation in the presence of phosphorescence and fluorescence, and he provided striking results generated with a modified version of the public domain raytracer *rayshade*. Sadly, this work was not followed up, nor was the modified version of rayshade made public. Also, we are not aware of any work that aims at considering the inclusion of fluorescence effects in sophisticated reflectance models.

4 A Combined Renderer

We first introduce an alternative notation that can be used for polarization support, and then show how this formalism can easily be combined with fluorescence support.

4.1 Alternative Polarization Support

A description for polarized radiation which due to its simpler mathematical characteristicsis is better suited for use in raytracing–based rendering systems is that of *Stokes parameters*. This description, while equivalent to coherency matrices, has the advantage of using only real–valued terms to describe all polarization states of optical radiation, and has an – also noncomplex – corresponding description of ray weights in the form of Müller matrices [11].
It has to be kept in mind that – similar to coherency matrices – both Stokes parameters and Müller matrices are meaningful only when considered within their own local reference frame; the main effect of this is that in a rendering system not only light, but also filters are *oriented* and have to store an appropriate reference in some way. However, for the sake brevity this spatial dependency is omitted in our following discussion except in the section about matrix realignment.

Stokes Parameters. Apart from coherency matrices, the polarization state of an electromagnetic wave of a given frequency can also be described in several other ways. Three real–valued parameters are required to describe a general polarization ellipse, but the *Stokes vector* notation defined by

$$\begin{aligned} E_{n,0} &= \kappa(V_x^2 + V_y^2) \qquad [W \cdot m^{-2}] \\ E_{n,1} &= \kappa(V_x^2 - V_y^2) \\ E_{n,2} &= \kappa(2V_x^2 \cdot V_y^2 \cdot \cos\gamma) \\ E_{n,3} &= \kappa(2V_x^2 \cdot V_y^2 \cdot \sin\gamma) \end{aligned} \tag{3}$$

has proven itself in the optical measurements community, and has the key advantage that the first component of this 4–vector is the unpolarized intensity of the light wave in question (i.e. the same quantity that a nonpolarizing renderer uses). Components 2 and 3 describe the preference of the wave towards linear polarization at zero and 45 degrees, respectively, while the fourth encodes preference for right–circular polarization. While the first component is obviously always positive, the values for the three latter parameters are bounded by $[-E_{n,0}, E_{n,0}]$; e.g. for an intensity $E_{n,0} = 2$, a value of $E_{n,3} = -2$ would indicate light which is totally left circularly polarized.

The – at least in comparison to coherency matrices – much more comprehensible relationship between the elements of a Stokes vector and the state of the wavetrain it describes is, amongst other things, very beneficial during the debugging stage of a polarizing renderer, since it is much easier to construct verifiable test cases.

Müller Matrices. Müller matrices (MM for short) are the data structure used to describe a filtering operation by materials that are capable of altering the polarization state of incident light represented by a Stokes vector. The general modifier for a 4–vector is a 4×4–matrix, and the structure of the Stokes vectors implies that the elements of such a matrix correspond to certain physical filter properties. As with Stokes vectors, the better comprehensibilty of these real–valued data structures is of considerable benefit during filter specification and testing.
The degenerate case of MM is that of a nonpolarizing filter; this could equally well be described by a simple reflection spectrum. For such a filter the corresponding MM is the identity matrix. A more practical example is the MM of an ideal linear polarizer T_{lin}, where the polarization axis is tilted by an angle of ϕ against the reference coordinate system of the optical path under consideration, and which has the form of

$$\mathrm{T}_{lin}(\phi) = \frac{1}{2}\begin{bmatrix} 1 & \cos 2\phi & \sin 2\phi & 0 \\ \cos 2\phi & \cos^2 2\phi & \sin 2\phi \cdot \cos 2\phi & 0 \\ \sin 2\phi & \sin 2\phi \cdot \cos 2\phi & \sin^2 2\phi & 0 \\ 0 & 0 & 0 & 0 \end{bmatrix}.$$

For the purposes of physically correct rendering it is important to know the MM which is caused by evaluation of the Fresnel terms in equation (2). For a given wavelength and intersection geometry (i.e. specified index of refraction and angle of incidence), the resulting terms $F_\perp$, $F_\parallel$, $\delta_\perp$ and $\delta_\parallel$ have to be used as

$$\mathrm{T}_{Fresnel} = \begin{bmatrix} A & B & 0 & 0 \\ B & A & 0 & 0 \\ 0 & 0 & C & -S \\ 0 & 0 & S & C \end{bmatrix},$$

where $A = (F_\perp + F_\parallel)/2$, $B = (F_\perp - F_\parallel)/2$, $C = \cos(\delta_\perp - \delta_\parallel)$ and $S = \sin(\delta_\perp - \delta_\parallel)$; $\delta_\perp - \delta_\parallel$ is the total retardance the incident wavetrain is subjected to.

Filter Rotation. In order to correctly concatenate a filter chain described in section 2.3 (which basically amounts to matrix multiplications of the MMs in the chain), we have to be able to re–align a MM to a new reference system, which amounts to rotating it along the direction of propagation to match the other operands.
Contrary to first intuition, directional realignment operations are *not* necessary along the path of a concatenated filter chain; the retardance component of a surface interaction is responsible for the alterations that result from changes in wavetrain direction.
Since in the case of polarized light a rotation by an angle of ϕ can only affect the second and third components of a Stokes vector (i.e. those components that describe the linear component of the polarization state), the appropriate rotation matrix $\mathrm{M}(\phi)$ has the form of

$$\mathrm{M}(\phi) = \begin{bmatrix} 1 & 0 & 0 & 0 \\ 0 & \cos 2\phi & \sin 2\phi & 0 \\ 0 & -\sin 2\phi & \cos 2\phi & 0 \\ 0 & 0 & 0 & 1 \end{bmatrix}. \tag{4}$$

Matrices of the same form are also used to rotate Müller matrices. In order to obtain the rotated version of a MM $T(0)$, $M(\phi)$ has to be applied in a way similar to that shown for CMMs, namely $T(\phi) = M(-\phi) \cdot T(0) \cdot M(\phi)$.
Apart from being useful to re–align a filter through rotation, the matrix M given in equation (4) is also the MM of an ideal *circular retarder*. Linearly polarized light entering a material of this type will emerge with its plane of polarization rotated by an angle of ϕ; certain materials, such as crystal quartz or dextrose, exhibit this property, which is also referred to as *optical activity*.

4.2 Rendering of Fluorescence Effects

Since fluorescence is a material property, its description only affects the filter data structure. Specifically, for a system which uses n samples to represent spectra, filter values of fluorescent substances have to be a re–radiation matrix (RRM) of $n \times n$ elements.
The fact that fluorescence only ever causes light to be re–radiated at *lower* wavelengths than those at which it is absorbed allows us to only consider the lower half of this matrix. In practice, we use the same reflection spectra as for normal materials, only augmented with a data structure that holds the area below the main diagonal. All filtering operations were adapted to handle the presence of this crosstalk component as a sticky property; even if only one filter in a concatenation chain has an off–diagonal component, the overall result has to be also fluorescent.

4.3 Combining Fluorescence and Polarization

Similar to the previous section, this is a problem which only concerns the filtering operations. Specifically, the question is in which way nonpolarizing $n \times n$ (or n plus sub–diagonal crosstalk of $(n \times (n-1))/2$) re–radiation matrix filters and $n \times (4 \times 4)$ reflectance spectra with Müller matrices as samples can be properly mixed.

Practical Considerations. Fortunately, the solution is straightforward. The key observation here is that light which is re–emitted by fluorescent molecules can be considered to be unpolarized for our purposes, since this kind of light interaction with pigments has no directional character. This means that, while the full combination of the two properties would require the rather unwieldy construct of a data structure with $n \times n \times 4 \times 4$ entries (a MM for each RRM entry), we can get by with using a much smaller entity.
Our combined filter data structure uses the same nonpolarizing crosstalk component as the plain fluorescence–aware filter described in the previous section, and just replaces the main diagonal reflection spectrum with its polarizing counterpart.
The only area where this change caused a considerable increase in complexity are the filter manipulation methods, which have to account for four possible states of each operand (fluorescent yes/no, polarizing yes/no) in each procedure.

5 Results

We implemented the proposed dual polarization and fluorescence support in the public domain rendering software under development at our institute, the Advanced Rendering Toolkit (ART for short).

Spectral Rendering in ART. In order to faciliate spectral rendering experiments, ART is capable of using various internal representations of spectra for computations that deal with light. For reference purposes, there also exist two simple models which use generic RGB or CIE XYZ triplets to describe light as colour values; this can be thought of as compatibility mode to most current raytracers. The available spectral representations have 8, 16, 45 or – for reference calculations – 450 nonoverlapping box samples; the latter two correspond to 10 and 1 nm samples.
While more sophisticated approaches to spectral representation than box samples have been demonstrated in the past, for example by Peercy [9], Rougeron and Peroche [10] or Sun et al. [13], but their usefulness in the context of a general–purpose rendering system has yet to be investigated, and the increase in efficiency offered by the proposed techniques so far does not seem promising enough to offset the higher code complexity and speed penalty incurred by their use.

Filters and Light. The first task was to introduce the distinction between filters and light – as described in the previous sections – throughout the raytracing code of ART; the previously used polymorphous colour data type had to be appropriately replaced by filter and light structures.
As an unasked–for fringe benefit of this quite substantial task it transpired that the entire rendering code became much clearer semantically through the introduction of this distinction; this might serve as an encouragement for others who face the same task.

Fluorescence. The filters were then extended so that they also became capable of encoding fluorescence information as described in section 4.2. The main work during this step was the alteration of the filter manipulation routines and development of specialized storage classes for fluorescent reflection data.

Polarization. In order to be able to make meaningful performance comparisons, and also to keep the option of using a faster renderer without polarization capabilities for the majority of users who do not need the feature, polarization support was implemented as an additional compile–time option in ART in a similar way as the original spectral representation choice.
For the non–polarizeable renderer the procedures for polarization support expand to NOPs, so no overhead is incurred, and for the polarization–aware renderer they are expanded as inline funtions.
Apart from additional large changes to the the light and filter manipulation code (which had already been fleshed out and pushed into one module during the first step), the major changes in this stage involved the introduction of the capability to store and manipulate the orientation of light and filter data structures during rendering processes.
Three sample images obtained with this hybrid renderer are shown in figure 4 at the end of this paper.

Optimization. The only computational optimization with respect to polarization that has been implemented in ART so far is that each instance of the light and filter data structures is tagged as to whether it actually describes polarized light or a polarizing filter. This makes it possible to use faster routines if both operands in a calculation involving lights and/or filters are not polarized (specifically, multiplication of the samples instead of matrix operations). If one of the operands is polarized or polarizing, then so is the result of the computation: polarization is a sticky property of light and filters.

This simple optimization leads to a polarization–aware renderer which is on average only $10 - 30$ percent slower than its plain counterpart for scenes which do not contain any polarizing surfaces, lightsources or materials. Since practically all scenes contain at least a certain percentage of objects and lightsources that do not exhibit any polarized or polarizing property, this shortcut actually improves the performance of the polarization–aware renderer for all but extreme scenes.
For scenes with large amounts of polarizing objects – like e.g. the example scene shown in figure 4 – the slowdown of the polarizeable version compared the plain renderer is naturally higher and depends strongly on the scene. The example in figure 4 exhibits a fairly typical slowdown of around 500 percent (30 vs. 150 seconds rendering time); in some rare cases we have observed even larger performance drops. This drastic increase in rendering time is the price one has to pay for increased physical accuracy, although we estimate that some additional performance could be gained from aggressive global optimization of the numeric code in our rendering system.

6 Conclusion

We presented a practical way to implement combined polarization and fluorescence support in the context of a modern rendering system. The key improvements over previous approaches are

- The use of Stokes vectors to describe both unpolarized an polarized light with a single, intuitive formalism.
- The use of Müller matrices to describe the polarizing effect of materials and surfaces in an understandable way that is complementary to Stokes vectors.
- The combination of these formalisms with fluorescence information into a single rendering system.

Our future research will concern itself with the efficiency of spectral rendering in general, and in particular the choice of the most suitable spectral representation for photorealistic rendering, a question for which a good answer that is generally valid has yet to be given. In the course of these investigations we plan to also take the aspect of if both polarization and fluorescence can be represented even more efficiently into account, and investigate as to whether and how the usually large similarity in polarization state amongst samples in a given light spectrum can be safely exploited to reduce storage and computation requirements.

Acknowledgements

We are grateful to Labsphere Inc. for generously making measurements of fluorescent samples available. We also want to thank Ferdinand Bammer, Thomas Theußl and Katharina Horrak for valuable discussions.

References

1. Max Born and Emil Wolf. *Principles of Optics*. The Macmillan Company, 1964.
2. R. L. Cook and K. E. Torrance. A reflectance model for computer graphics. *Computer graphics, Aug 1981*, 15(3):307–316, 1981.

3. Andrew Glassner. A model for fluorescence and phosphorescence. In *Fifth Eurographics Workshop on Rendering*, pages 57–68, Darmstadt, Germany, June 1994. Eurographics.
4. Roy A. Hall and Donald P. Greenberg. A testbed for realistic image synthesis. *IEEE Computer Graphics and Applications*, 3(8):10–20, November 1983.
5. Xiao D. He, Kenneth E. Torrance, François X. Sillion, and Donald P. Greenberg. A comprehensive physical model for light reflection. *Computer Graphics*, 25(4):175–186, July 1991.
6. G. P. Können. *Polarized Light in Nature*. Cambridge University Press, 1985.
7. M. Minnaert. *Light and Color in the Open Air*. Dover, 1954.
8. G. B. Parrent and P. Roman. On the matrix formulation of the theory of partial polarization in terms of observables. *Il Nuovo Cimento (English version)*, 15(3):370–388, February 1960.
9. Mark S. Peercy. Linear color representations for full spectral rendering. In James T. Kajiya, editor, *Computer Graphics (SIGGRAPH '93 Proceedings)*, volume 27, pages 191–198, August 1993.
10. Gilles Rougeron and Bernard Péroche. An adaptive representation of spectral data for reflectance computations. In Julie Dorsey and Philipp Slusallek, editors, *Eurographics Rendering Workshop 1997*, pages 127–138, New York City, NY, June 1997. Eurographics, Springer Wien. ISBN 3-211-83001-4.
11. John B. Shumaker. Distribution of optical radiation with respect to polarization. In Fred E. Nicodemus, editor, *Self–Study Manual on Optical Radiation Measurements, Part 1: Concepts*. Optical Physics Division, Institute for Basic Standards, National Bureau of Standards, Washington, D.C., June 1977.
12. Robert Siegel and John R. Howell. *Thermal Radiation Heat Transfer, 3rd Edition*. Hemisphere Publishing Corporation, New York, NY, 1992.
13. Yinlong Sun, F. David Fracchia, and Mark S. Drew. A composite model for representing spectral functions. Technical Report TR 1998-18, School of Computing Science, Simon Fraser University, Burnaby, BC, Canada, November 1998.
14. David C. Tannenbaum, Peter Tannenbaum, and Michael J. Wozny. Polarization and birefringency considerations in rendering. In Andrew Glassner, editor, *Proceedings of SIGGRAPH '94 (Orlando, Florida, July 24–29, 1994)*, Computer Graphics Proceedings, Annual Conference Series, pages 221–222. ACM SIGGRAPH, ACM Press, July 1994. ISBN 0-89791-667-0.
15. Turner Whitted. An improved illumination model for shaded display. *IEEE Computer Graphics & Applications*, 23(6):343–349, June 1980.
16. Lawrence B. Wolff and David Kurlander. Ray tracing with polarization parameters. *IEEE Computer Graphics & Applications*, 10(6):44–55, November 1990.

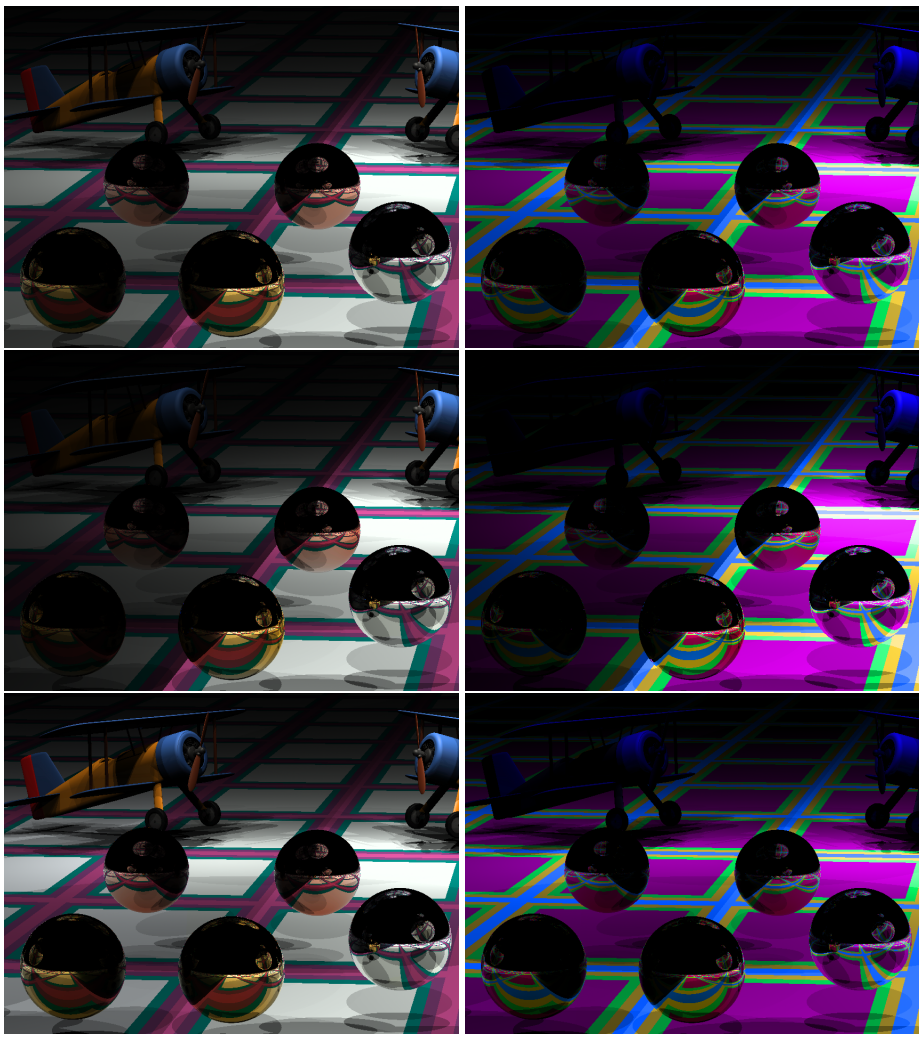

Fig. 4. Example renderings of polarization effects combined with fluorescent objects. The left and right columns show similar setups under two different illuminations - at the left D65, and at the right UV blacklight. The scene shows several metal spheres (gold, copper, silver) and a nonfluorescent object (the biplane model) which float over a diffuse floor with fluorescent properties, and which are reflected in a large block of a dieelectric material (glass). The reflection is viewed well below Brewster's angle in order to increase its intensity; because of this, the polarizing filters which are placed in front of the camera in the two lower images (horizontal polarizer in the middle, vertical at the bottom) do not affect the entire reflected energy. For comparison purposes, the topmost two images have a 50 percent neutral grey filter instead of a polarizer placed in front of the camera. These images can also be viewed in higher resolution at http://www.artoolkit.org/Gallery/Fluorescence/.